JOURNAL OF CATALYSIS 106, 362–368 (1987)

Spectroscopic Characterization of TiO_2/Al_2O_3 and Co/Al_2O_3–TiO_2 Catalysts

MICHAEL A. STRANICK, MARWAN HOUALLA, AND DAVID M. HERCULES

Department of Chemistry, University of Pittsburgh, Pittsburgh, Pennsylvania 15260

Received September 2, 1986; revised March 10, 1987

X-ray photoelectron spectroscopy (ESCA or XPS), laser Raman spectroscopy (LRS), and X-ray diffraction (XRD) have been used to characterize the dispersion and chemical state of a series of TiO_2/Al_2O_3 carriers and a series of 3% Co/Al_2O_3–TiO_2 catalysts. It was found that titania is well dispersed on alumina for Ti loadings less than 14 wt%. The formation of a $TiO_2:Al_2O_3$ surface phase occurred for carriers in the 1 to 6 wt% Ti range. Formation of anatase occurred, in addition to the $TiO_2:Al_2O_3$ surface phase, at loadings in excess of 6 wt% Ti, with the amount of anatase increasing with increasing titania loading. ESCA data indicate that the dispersion of cobalt supported on the titania-modified alumina carriers increased with increasing titania loading. XRD and LRS results show that the increase in dispersion can, in part, be ascribed to the formation of a surface cobalt phase at the detriment of the Co_3O_4 phase.

INTRODUCTION

Recent work has shown that the nature of the carrier can have a dramatic influence on the chemical properties and activity of a supported metal catalyst (*1–5*). Particular emphasis has been placed on studying the behavior of metals supported on reducible carriers (*6–11*). One problem encountered in these studies is that the dispersion of the active phase often varies with the type of carrier used. This would lead to ambiguity in separating the role of the carrier from the effect of active phase particle size. As a result, there is interest in studying the use of supported oxides, such as La_2O_3 or CeO_2, as "promoters" on high-surface-area carriers, Al_2O_3 or SiO_2, for example (*12*). Furthermore, it is believed that the uniform deposition of a reducible carrier on a nonreducible support may permit a systematic study of the SMSI (strong metal–support interaction) effect (*13–16*).

To fully understand the effect of a supported oxide carrier on an active phase, the chemical state and dispersion of the supported oxide must first be known. Previously published work on TiO_2–Al_2O_3, Nb_2O_5–SiO_2, and TiO_2–SiO_2 supported oxide systems has relied on only X-ray diffraction and transmission electron microscopy to infer the dispersions of the titania or niobia phases (*13–16*). Questions regarding the chemical nature of the titania or niobia phases were not fully addressed. In the present work, X-ray photoelectron spectroscopy and laser Raman spectroscopy have been used to gain better insight into the chemical state and dispersion of titania supported on alumina. In addition, since titania has been used as an additive in hydrodesulfurization and CO hydrogenation catalysts (*17, 18*), the present work also reports the effects of titania on the chemical state and dispersion of a Co/Al_2O_3 catalyst.

EXPERIMENTAL

Catalyst Preparation

A series of titania-modified alumina carriers was prepared by nonaqueous impregnation of γ-Al_2O_3 (Harshaw Chemical Co., Al-1401P, BET surface area, 180 m^2/g; pore volume, 0.43 ml/g) with solutions of titanium(IV) isopropoxide, $Ti(O\text{-}iPr)_4$ (Aldrich

0021-9517/87 $3.00

Chemical Co.), dissolved in spectrophotometry grade 2-propanol (J. T. Baker). An appropriate amount (7.8 to 62 vol%) of $Ti(O\text{-}iPr)_4$ was dissolved in a volume of 2-propanol such that the total solution volume was equal to approximately twice the pore volume of the support. Modified supports having titania loadings from 1 to 14 wt% as Ti were prepared. Supports containing greater than 8 wt% Ti were prepared by double impregnation of the alumina using one-half the requisite amount of $Ti(O\text{-}iPr)_4$. Following impregnation the alumina was placed in moist air at room temperature for 2 h to facilitate hydrolysis of the $Ti(O\text{-}iPr)_4$. The titania-modified aluminas were dried under ambient conditions for 48 h, followed by further drying in air at 120°C for 4 h. The modified carriers were then calcined in air at 600°C for 6 h. The nitrogen BET surface areas of the 2 to 14 wt% Ti-modified carriers were approximately 25 ± 5 m^2/g less than titania-free alumina. There was no significant variation in surface area among the titania-modified carriers in the 2 to 14 wt% Ti range. The decrease in surface area observed in this study for titania-modified alumina is consistent with results reported by others (*13*).

Cobalt was deposited on the titania-modified aluminas by aqueous pore volume impregnation using cobalt nitrate (J. T. Baker) solutions. A constant cobalt loading of 3 wt% (of the Al_2O_3) as Co metal was employed. Cobalt catalysts were dried and calcined in air at 120°C for 16 h and at 400°C for 6 h, respectively. The modified carriers and the cobalt catalysts were finely ground (approx. 180 mesh) to minimize the effects of sample inhomogeneity on surface analysis.

Catalyst Characterization

X-ray diffraction (XRD). X-ray diffraction patterns of catalyst samples were obtained with a Diano 700 diffractometer, which utilizes nickel-filtered Cu$K\alpha$ radiation. Diffraction patterns were obtained with the X-ray gun operated at 50 kV and 25 mA, using a scan rate of 0.4° min^{-1} (2θ). Samples were run as powders mounted in a plastic holder. Compound identification was accomplished through comparison of measured spectra with ASTM powder diffraction file data.

Laser Raman spectroscopy (LRS). Laser Raman spectra were obtained with a Spex Ramalog spectrometer which utilizes holographic gratings. The excitation source was the 514.5-nm line from a Spectra-Physics argon-ion laser, which delivered approximately 25 mW of power measured at the sample. Reported peaks are accurate to within ±2 cm^{-1}. Samples were pressed into pellets with a KBr support and rotated off axis to prevent excessive heating by the laser beam.

X-ray photoelectron spectroscopy (ESCA or XPS). X-ray photoelectron spectra of catalyst samples were obtained with a Leybold–Heraeus LHS-10 surface analysis system interfaced to a Hewlett–Packard 1000 computer. The LHS-10 instrument was operated in the fixed analyzer transmission mode. In the present study, an aluminum anode (Al$K\alpha$ = 1486.6 eV) operated at 12 kV and 20 mA was employed. The residual pressure inside the spectrometer was 10^{-8} Torr or lower. ESCA measurements were done on catalyst powders which had been dusted onto double-sided adhesive tape and mounted on the spectrometer probe. Measurements were made on freshly calcined catalysts to minimize the level of carbon contamination on the catalyst samples.

It has been shown that the ESCA intensity ratio of supported phase and carrier peaks is related to the dispersion of the supported phase (*19–21*). In the present work, the intensity ratios predicted for monolayer supported phase coverage were calculated using the model of Kerkhof and Moulijn (*21*). Photoelectron cross sections and escape depths used in the calculation were obtained from Scofield (*22*) and Penn (*23*), respectively. Experimental ESCA intensity ratios were reproducible to within

±10% r.s.d. or better. Photoelectron peak intensities were determined following linear background subtraction.

ESCA binding energies of catalyst samples were referenced to the Al 2*p* line at 74.5 eV. The Al 2*p* binding energy was previously determined through deposition of gold onto γ-alumina and referencing to the Au $4f_{7/2}$ line at 83.8 eV (*24*). The binding energies of standard compounds were referenced to the C 1*s* line at 284.6 eV. The C 1*s* peak measured from catalyst samples averaged 284.6 eV, referenced to the Al 2*p* line. Binding energy values were measured with a precision of ±0.2 eV or better.

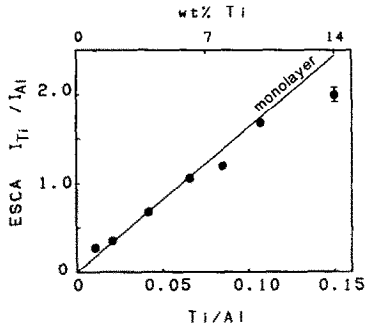

FIG. 1. ESCA Ti 2*p*/Al 2*s* intensity ratios of TiO_2/Al_2O_3 carriers plotted versus Ti/Al atomic ratio (points). Ti 2*p*/Al 2*s* intensity ratios calculated for monolayer TiO_2 coverage (line).

RESULTS AND DISCUSSION

Titania-Modified Alumina

X-ray powder diffraction analysis of the titania-modified carriers revealed no diffraction lines other than those of the alumina for samples having Ti loadings less than 14 wt%. The sample containing 14 wt% Ti exhibited a weak line characteristic of the anatase form of TiO_2. Thus, formation of well crystallized TiO_2 occurs at a Ti loading of 14 wt%. By comparison of the intensity of the $2\theta = 48°$ anatase diffraction line from the modified carrier with those exhibited by anatase–alumina physical mixtures, it was determined that approximately 1.5 wt% Ti is present as well crystallized anatase (particle size greater than ca. 4 nm) for the 14 wt% Ti catalyst.

The ESCA Ti $2p_{3/2}$ binding energies of the TiO_2/Al_2O_3 series were invariant with titania loading and averaged 459.1 ± 0.1 eV. The measured Ti $2p_{3/2}$ binding energy value of the modified carriers was consistent with that measured for TiO_2, 459.0 eV (*25*). Figure 1 shows the ESCA Ti 2*p*/Al 2*s* intensity ratios plotted as a function of Ti/Al atomic ratio. Also shown in Fig. 1 is the line corresponding to the Ti/Al intensity ratios predicted for monolayer titania coverage calculated using the Kerkhof–Moulijn model. The decrease in surface area of the support resulting from titania impregnation was taken into account in calculating the monolayer values (*21*). The measured intensity ratios of the TiO_2/Al_2O_3 carriers were consistent with those predicted by the monolayer model for titania loadings below a Ti/Al atomic ratio of 0.15 (14 wt% Ti), indicating a highly dispersed titania phase. The measured intensity ratio of the 14 wt% Ti carrier was below the predicted monolayer value, indicating that some fraction of the titania is present in the form of particles or islands. This result correlates with the appearance of anatase lines in the XRD pattern of the 14 wt% Ti carrier.

Laser Raman analysis of the modified aluminas having titania loadings less than 8 wt% Ti were similar to the Raman spectrum of unmodified alumina (*26*), as no Raman bands were observed. The laser Raman spectrum of the 6 wt% Ti alumina, shown in Fig. 2A, is typical for those carriers having Ti loadings less than 8 wt%. Modified aluminas having titania loadings of 8 wt% Ti and greater exhibited bands due to anatase. The Raman spectra of carriers containing titania loadings of 8 and 14 wt% Ti are shown in Figs. 2B and 2C. The Raman bands at 401, 515, and 641 cm^{-1} are characteristic of anatase (*27*). The rutile form of TiO_2 was not detected for the modified carriers at any titania loading studied. The intensities of the TiO_2 bands

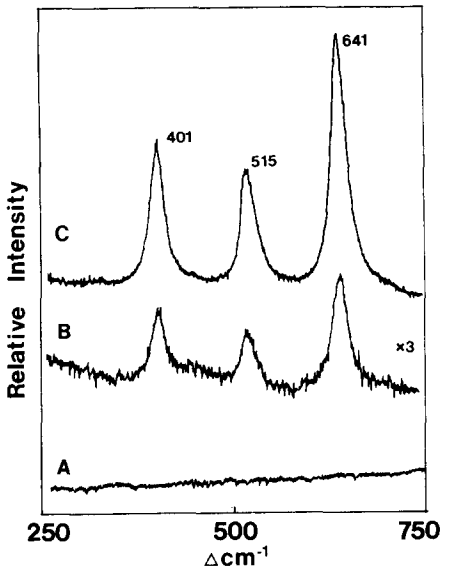

FIG. 2. Laser Raman spectra of TiO_2/Al_2O_3 supports containing (A) 6 wt% Ti, (B) 8 wt% Ti, and (C) 14 wt% Ti.

increased with increasing titania loading, for the modified carriers in the 8 to 14 wt% Ti range, indicating an increase in the amount of anatase. The amount of anatase present on the modified carriers was estimated by comparison of the band intensities for the modified carriers with those from anatase–alumina physical mixtures. Table 1 presents the amounts of anatase present on the TiO_2/Al_2O_3-modified carriers. It can be seen that of the titania present on the 8 wt% Ti-modified carrier, 0.2 wt% was present as anatase. Similarly, for the 10 and 14 wt% Ti-modified aluminas, the anatase content was 0.4 and 2 wt%, respectively.

The previous results illustrate that combined use of XRD, LRS, and ESCA is needed to achieve a comprehensive characterization of the TiO_2/Al_2O_3 system. X-ray diffraction analysis of titania-modified alumina revealed that titania is present either in a well-dispersed or an amorphous state at loadings below 14 wt%, with segregation of crystalline anatase particles at a loading of 14 wt% Ti. Surface characterization of the titania-modified aluminas indicated that titania is highly dispersed, at loadings below 14 wt% Ti. From the Raman spectra of the modified carriers containing 6 wt% Ti and less, it can be concluded that titania is probably present in the form of a Raman-inactive TiO_2: Al_2O_3 surface phase, perhaps a surface aluminum titanate. Raman analysis also indicated that at titania loadings greater than 6 wt% Ti, anatase formation occurred. The ESCA results were consistent with results from XRD and LRS analyses in regard to the dispersion of the titania phases, for modified carriers having titania loadings of 8 wt% Ti and greater. For the 8 and 10 wt% Ti-modified carriers, the fraction of anatase estimated by LRS was small. Hence, the presence of any discrete anatase particles would not be reflected by a decrease in the ESCA intensity ratios, relative to the monolayer values. For the 14 wt% Ti-modified alumina, the amount of crystalline anatase present was approximately 1.5 to 2 wt% as estimated by XRD and LRS. The lower ESCA Ti/Al intensity ratio of the 14 wt% Ti carrier, relative to the monolayer value, can be accounted for by a mean particle size of 10 nm for the anatase fraction, using a calculation based on Kerkhof and Moulijn (*21*) and assuming ±10% error.

Co/Al_2O_3–TiO_2

X-ray diffraction analysis of the titania-free, 3% Co/Al_2O_3 catalyst revealed diffraction lines due to Co_3O_4. Diffraction patterns of the 3% Co/Al_2O_3 catalysts in the 1 to 4 wt% Ti range also exhibited Co_3O_4 lines with intensities similar to those of the unmodified carrier. The intensity of the Co_3O_4 diffraction lines decreased with

TABLE 1

Percentage of Anatase in TiO_2/Al_2O_3 Carriers Estimated by Laser Raman Spectroscopy

wt% Ti	1	2	4	6	8	10	14
wt% Ti present as anatase	0	0	0	0	0.2	0.4	1.9

increasing titania loading for samples with Ti contents greater than 4 wt%, indicating a decrease in the amount of crystalline Co_3O_4. Catalysts having titania loadings of 10 wt% Ti and greater exhibited no diffraction lines characteristic of cobalt compounds, indicating the absence of crystalline cobalt species of approximately 4-nm or greater particle size.

The ESCA Co $2p_{3/2}$ binding energies of the Co/Al_2O_3–TiO_2 catalysts were invariant with titania loading and averaged 781.9 ± 0.1 eV. The measured binding energies and satellite structure were typical of 3% Co/Al_2O_3 catalysts and indicated the presence of a cobalt surface phase (Co^{2+} in tetrahedral and octahedral environments) on the catalyst (*24*). The Co $2p_{3/2}$ binding energies reflect the presence of the cobalt surface phase and not Co_3O_4, because of differences in dispersion of the Co_3O_4 and cobalt surface phases. The Co_3O_4 phase is present as large crystallites (as evidenced by XRD), while the cobalt surface phase is well dispersed. As a result of this difference in dispersion, the fraction of the Co_3O_4 phase which is detected by ESCA is small relative to that of the cobalt surface phase and hence, the Co $2p_{3/2}$ binding energies of the catalysts will reflect that of the cobalt surface phase (*28*). Figure 3 shows the ESCA Co $2p_{3/2}$/Al 2*s* intensity ratios plotted as a function of titania loading for Co/Al_2O_3–TiO_2 catalysts. Also shown is the intensity ratio predicted for monolayer cobalt coverage based on the Kerkhof–Moulijn model, taking into account the decrease in support surface area (*21*). The Co/Al intensity ratios of catalysts having Ti/Al atomic ratios of 0.02 (2 wt% Ti) and less do not differ from the intensity ratio of the unmodified Co/Al_2O_3 catalyst. Catalysts having titania loadings larger than a Ti/Al atomic ratio of 0.02 (2 wt%) exhibited a linear increase in the Co/Al intensity ratio with increasing titania loading. This increase in intensity ratio indicates that the presence of titania causes either an increase in cobalt dispersion or a redistribution of cobalt to the external portions of the support particles. The measured intensity ratios for low titania contents were well below the value predicted for monolayer cobalt coverage. However, the experimental intensity ratios approached the monolayer value for catalysts with increasing titania contents. The ESCA Ti $2p_{3/2}$ binding energies and Ti/Al intensity ratios were unaffected (±0.1 eV and ±5%, respectively) by cobalt impregnation.

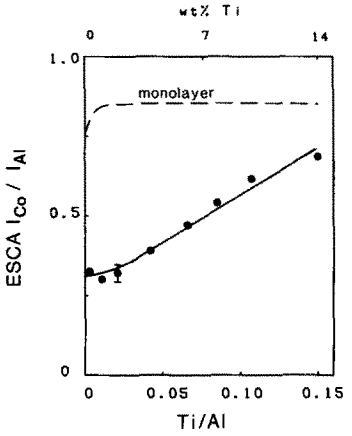

FIG. 3. ESCA Co $2p_{3/2}$/Al 2*s* intensity ratios of 3% $Co/Al_2O_3/TiO_2$ catalysts plotted as a function of Ti/Al atomic ratio (solid line). Co $2p_{3/2}$/Al 2*s* intensity ratio calculated assuming monolayer Co coverage (broken line).

Laser Raman spectra from the 3% Co/Al_2O_3–TiO_2 catalyst series containing 0, 8, and 14 wt% Ti are shown in Fig. 4A–4C. It can be seen that Co_3O_4 is present on all catalysts, as evidenced by Raman bands at 693, 524, and 485 cm^{-1} (*29*). As noted in the case of the TiO_2/Al_2O_3 carriers, Raman bands at 401, 515, and 641 cm^{-1} due to anatase were observed for the 8 to 14 wt% Ti catalysts. Figure 5 shows the intensity of the 693-cm^{-1} Co_3O_4 band plotted as a function of Ti loading for the 3 wt% Co/Al_2O_3–TiO_2 catalysts. Catalysts having titania loadings of 2 wt% and less exhibited similar Co_3O_4 band intensities, indicating that low titania loadings had no effect on the amount of Co_3O_4. For catalysts with higher titania loadings, the intensities of the

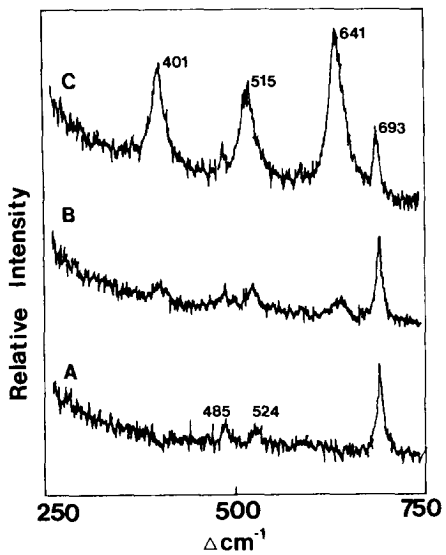

FIG. 4. Laser Raman spectra of 3% Co/Al_2O_3–TiO_2 catalysts containing (A) 0 wt% Ti, (B) 8 wt% Ti, and (C) 14 wt% Ti.

Co_3O_4 bands decreased with increasing titania content, indicating clearly that the presence of titania suppresses the formation of Co_3O_4. The Co_3O_4 band intensity decreased by approximately a factor of 2 for the 14 wt% Ti catalyst, relative to the unmodified material. The Raman spectrum of $CoTiO_3$ was measured for reference purposes, with the most intense band occurring at 703 cm^{-1}. $CoTiO_3$ was not detected on any of the titania-modified catalysts as indicated by the absence of the 703-cm^{-1} band.

In summary, ESCA characterization of 3% Co/Al_2O_3–TiO_2 catalysts revealed that

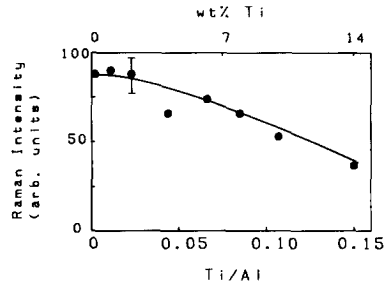

FIG. 5. Absolute intensity of 693-cm^{-1} Co_3O_4 Raman band versus Ti/Al atomic ratio for 3% Co/Al_2O_3–TiO_2 catalysts (±15% r.s.d.).

for titania loadings greater than 2 wt% Ti, Co/Al intensity ratios increased with increasing titania loading. Laser Raman spectroscopy indicated that Co_3O_4 was present on all the catalysts with the amount of Co_3O_4 decreasing with increasing titania loading. X-ray diffraction results also indicated a decrease in Co_3O_4 content with increasing titania loading. The decrease in Co_3O_4 content observed by LRS and XRD indicates that a redistribution of Co_3O_4 from within the support pore structure to the exterior of the support particles is not responsible for the increase in the ESCA Co/Al intensity ratios. Thus, the increase in Co/Al intensity ratios can be attributed to an increase in Co dispersion resulting from the formation of a highly dispersed surface $Co : Al_2O_3$–TiO_2 phase at the detriment of the Co_3O_4 phase.

CONCLUSIONS

1. X-ray diffraction and ESCA data reveal that titania is well dispersed on the surface of γ-Al_2O_3 for carriers with loadings below 14 wt% Ti. ESCA and LRS data suggest that for loadings of 1 to 6 wt%, titania is present in the form of a $TiO_2 : Al_2O_3$ surface phase. The formation of anatase occurs for loadings in excess of 6 wt% Ti.

2. ESCA results indicate that the dispersion of 3% cobalt supported on γ-Al_2O_3 modified with titania increases with increasing titania loading. From XRD and laser Raman data it can be concluded that the increase in Co dispersion is due in part to the formation of a $Co : Al_2O_3$–TiO_2 surface phase at the detriment of the Co_3O_4 phase.

3. The present work demonstrates that the use of several complementary techniques is necessary for determining the dispersion and chemical state of supported oxide systems.

ACKNOWLEDGMENTS

The authors acknowledge financial support for this work from the U.S. Department of Energy, Grant

DE-AC02-79ER10485. M.A.S. acknowledges SOHIO for a graduate fellowship.

REFERENCES

1. Ng, K. Y. S., and Gulari, E., *J. Catal.* **92,** 340 (1985).
2. Ng, K. Y. S., and Gulari, E., *J. Catal.* **95,** 33 (1985).
3. Bartholomew, C. H., and Reuel, R. C., *J. Catal.* **85,** 78 (1984).
4. Bartholomew, C. H., and Vance, G. K., *J. Catal.* **91,** 78 (1985).
5. Vannice, M. A., Twu, C. C., and Moon, S. A., *J. Catal.* **79,** 70 (1983).
6. Tauster, S. J., Fung, S. C., and Garten, R. L., *J. Amer. Chem. Soc.* **100,** 170 (1978).
7. Tauster, S. J., and Fung, S. C., *J. Catal.* **55,** 29 (1978).
8. Resasco, D. E., and Haller, G. L., *J. Catal.* **82,** 279 (1983).
9. Simeons, A. J., Baker, R. T. K., Dwyer, D. J., Lund, C. R. F., and Madon, R. J., *J. Catal.* **86,** 359 (1984).
10. Ko, E. I., Hupp, J. M., Rogan, F. H., and Wagner, N. J., *J. Catal.* **84,** 85 (1983).
11. Singh, A. K., Pande, N. K., and Bell, A. T., *J. Catal.* **94,** 422 (1985).
12. Reick, J. S., and Bell, A. T., *J. Catal.* **99,** 278 (1986).
13. McVicker, G. B., and Ziemiak, J. J., *J. Catal.* **95,** 473 (1985).
14. Ko, E. I., Bafrali, R., Nuhfer, N. T., and Wagner, N. J., *J. Catal.* **95,** 260 (1985).
15. Murrell, L. L., and Yates, D. J. C., *Stud. Surf. Sci. Catal.* **7,** 1470 (1981).
16. Ko, E. I., and Wagner, N. J., *J. Chem. Soc. Chem. Commun.* **19,** 1274 (1984).
17. Houalla, M., Kibby, C. L., Eddy, E. L., Petrakis, L., and Hercules, D. M., *in* "Proceedings, 8th Intl. Cong. Catal.," Vol. IV, p. 359. Elsevier, Amsterdam, 1984.
18. Reick, J. S., and Bell, A. T., *J. Catal.* **99,** 262 (1986).
19. Defosse, C., Canesson, P., Rouxhet, P., and Delmon, B., *J. Catal.* **51,** 269 (1978).
20. Fung, S. C., *J. Catal.* **58,** 454 (1979).
21. Kerkhof, F. P. J. M., and Moulijn, J. A., *J. Phys. Chem.* **83,** 1612 (1979).
22. Scofield, J. H., *J. Elec. Spectrosc. Relat. Phenom.* **8,** 129 (1976).
23. Penn, D. R., *J. Elec. Spectrosc. Relat. Phenom.* **9,** 29 (1976).
24. Chin, R. L., and Hercules, D. M., *J. Phys. Chem.* **86,** 360 (1982).
25. Raupp, G. B., and Dumesic, J. A., *J. Phys. Chem.* **89,** 5240 (1985).
26. Zingg, D. S., Makovsky, L. E., Tischer, R. E., Brown, F. R., and Hercules, D. M., *J. Phys. Chem.* **84,** 2898 (1980).
27. Balachandran, U., and Eror, N. G., *J. Solid State Chem.* **42,** 276 (1982).
28. Stranick, M. A., Houalla, M., and Hercules, D. M., *J. Catal.* **103,** 151 (1987).
29. Jeziorowski, J., Knozinger, H., Grange, P., and Gajardo, P., *J. Phys. Chem.* **84,** 1825 (1980).